University of Groningen

Impact of Coronary Computerized Tomography Angiography-Derived Plaque Quantification and Machine-Learning Computerized Tomography Fractional Flow Reserve on Adverse Cardiac Outcome

Doeberitz, Philipp L. von Knebel; De Cecco, Carlo N.; Schoepf, U. Joseph; Albrecht, Moritz H.; van Assen, Marly; De Santis, Domenico; Gaskins, Jeffrey; Martin, Simon; Bauer, Maximilian J.; Ebersberger, Ullrich

IMPORTANT NOTE: You are advised to consult the publisher's version (publisher's PDF) if you wish to cite from it. Please check the document version below.

Document Version
Publisher's PDF, also known as Version of record

Citation for published version (APA):
Doeberitz, P. L. V. K., De Cecco, C. N., Schoepf, U. J., Albrecht, M. H., van Assen, M., De Santis, D., Gaskins, J., Martin, S., Bauer, M. J., Ebersberger, U., Giovagnoli, D. A., Varga-Szemes, A., Bayer, R. R., Schoenberg, S. O., & Tesche, C. (2019). Impact of Coronary Computerized Tomography Angiography-Derived Plaque Quantification and Machine-Learning Computerized Tomography Fractional Flow Reserve on Adverse Cardiac Outcome. *American Journal of Cardiology*, *124*(9), 1340-1348. https://doi.org/10.1016/j.amjcard.2019.07.061

Impact of Coronary Computerized Tomography Angiography-Derived Plaque Quantification and Machine-Learning Computerized Tomography Fractional Flow Reserve on Adverse Cardiac Outcome

Philipp L. von Knebel Doeberitz, MD[a,b], Carlo N. De Cecco, MD, PhD[a,c], U. Joseph Schoepf, MD[a,d,*],
Moritz H. Albrecht, MD[a,e], Marly van Assen, MSc[a,f], Domenico De Santis, MD[a,g],
Jeffrey Gaskins, BSc[a], Simon Martin, MD[a,e], Maximilian J. Bauer, MEd[a], Ullrich Ebersberger, MD[a,h,i],
Dante A. Giovagnoli, MS[a], Akos Varga-Szemes, MD, PhD[a], Richard R. Bayer, 2nd, MD[a,d],
Stefan O. Schönberg, MD[b], and Christian Tesche, MD[a,i,j]

This study investigated the impact of coronary CT angiography (cCTA)-derived plaque markers and machine-learning-based CT-derived fractional flow reserve (CT-FFR) to identify adverse cardiac outcome. Data of 82 patients (60 ± 11 years, 62% men) who underwent cCTA and invasive coronary angiography (ICA) were analyzed in this single-center retrospective, institutional review board-approved, HIPAA-compliant study. Follow-up was performed to record major adverse cardiac events (MACE). Plaque quantification of lesions responsible for MACE and control lesions was retrospectively performed semiautomatically from cCTA together with machine-learning based CT-FFR. The discriminatory value of plaque markers and CT-FFR to predict MACE was evaluated. After a median follow-up of 18.5 months (interquartile range 11.5 to 26.6 months), MACE was observed in 18 patients (21%). In a multivariate analysis the following markers were predictors of MACE (odds ratio [OR]): lesion length (OR 1.16, p = 0.018), low-attenuation plaque (<30 HU) (OR 4.59, p = 0.003), Napkin ring sign (OR 2.71, p = 0.034), stenosis ≥50% (OR 3.83, p 0.042), and CT-FFR ≤0.80 (OR 7.78, p = 0.001). Receiver operating characteristics analysis including stenosis ≥50%, plaque markers and CT-FFR ≤0.80 (Area under the curve 0.94) showed incremental discriminatory power over stenosis ≥50% alone (Area under the curve 0.60, p <0.0001) for the prediction of MACE. cCTA-derived plaque markers and machine-learning CT-FFR demonstrate predictive value to identify MACE. In conclusion, combining plaque markers with machine-learning CT-FFR shows incremental discriminatory power over cCTA stenosis grading alone.   © 2019 Elsevier Inc. All rights reserved. (Am J Cardiol 2019;124:1340−1348)

Coronary computed tomography angiography (CTA) has evolved to being an accepted method to rule out obstructive coronary artery disease (CAD) and enables direct noninvasive atherosclerotic plaque assessment.[1,2] Obstructive CAD, defined by luminal diameter reduction of ≥50%, alongside several plaque features have demonstrated prognostic power for the prediction of major adverse cardiac events (MACE) beyond traditional cardiovascular risk factors.[3,4] More recently, cCTA-derived fractional flow reserve (CT-FFR) utilizing a machine-learning based approach has been introduced and validated against invasive FFR as a robust method for the identification of lesion-specific ischemia.[5−7] However, the potential of noninvasive cCTA-derived plaque quantification combined with machine-learning based CT-FFR for the prediction of MACE requires further investigation. In the present study, thus, we sought to investigate the impact of cCTA-derived plaque quantification and machine-learning based CT-FFR to identify MACE.

This study was approved by the institutional review board and the need for written informed consent was waived due to the retrospective nature of this investigation. The study was performed in full HIPAA compliance. We retrospectively analyzed data of a patient cohort with known or suspected CAD who underwent cCTA and

[a]Division of Cardiovascular Imaging, Department of Radiology and Radiological Science, Medical University of South Carolina, Charleston, South Carolina; [b]Institute of Clinical Radiology and Nuclear Medicine, University Medical Center Mannheim, Medical Faculty Mannheim-Heidelberg University, Mannheim, Germany; [c]Division of Cardiothoracic Imaging, Nuclear Medicine and Molecular Imaging, Department of Radiology and Imaging Sciences, Emory University Hospital, Atlanta, Georgia; [d]Division of Cardiology, Department of Medicine, Medical University of South Carolina, Charleston, South Carolina; [e]Department of Diagnostic and Interventional Radiology, University Hospital Frankfurt, Frankfurt, Germany; [f]Center for Medical Imaging North East Netherlands, University Medical Center Groningen, University of Groningen, Groningen, The Netherlands; [g]Department of Radiological Sciences, Oncology and Pathology, University of Rome "Sapienza", Rome, Italy; [h]Kardiologie MVZ München-Nord, Munich, Germany; [i]Department of Cardiology, Munich University Clinic, Ludwig-Maximilians-University, Munich, Germany; and [j]Department of Internal Medicine, St. Johannes-Hospital, Dortmund, Germany. Manuscript received June 19, 2019; revised manuscript received and accepted July 18, 2019.

See page 1346 for disclosure information.

*Corresponding author: Tel: (843) 876-7146; fax: (843) 876-3157.

E-mail address: schoepf@musc.edu (U.J. Schoepf).

invasive coronary angiography (ICA) between October 2012 and July 2017. Follow-up for the occurrence of MACE was performed for a maximum of 36 months. MACE were defined as cardiac death (fatal myocardial infarction [MI]), nonfatal MI (ST-segment elevation and non-ST-segment elevation MI), and unstable angina leading to coronary revascularization (percutaneous coronary intervention or coronary artery bypass grafting) with more than 6 weeks between cCTA and ICA with the revascularization procedure.[8] The patients' Framingham risk score was calculated to reflect clinical risk for cardiovascular events. Portions of the included population have been reported on in a previous study.[9] Patients with previous myocardial infarction, previous percutaneous coronary stent implantation or coronary artery bypass grafting, severely reduced left ventricular function (ejection fraction ≤30%), and bifurcation stenosis were excluded from further analysis. Nondiagnostic cCTA image quality also led to exclusion. Patient baseline characteristics and risk factors were obtained from medical records. Patients fulfilling the inclusion criteria were followed up by using electronic medical records of the hospital, data obtained from the United States Social Security Death Index, and patient phone calls. The primary outcome was MACE, a composite of cardiac death, MI, unstable angina, and coronary revascularization later than 90 days after the initial cCTA. Cardiac death was defined as mortality due to MI, ventricular arrhythmias, heart failure, or cardiogenic shock. MI was defined using the above-described criteria. An independent cardiologist blinded to cCTA imaging results interpreted all clinical information, including electrocardiogram (ECG), laboratory results, echocardiography, and ICAs for definition of MACE.

cCTA acquisition was achieved using either first, second, or third generation dual-source CT (DSCT) scanner (SOMATOM Definition, SOMATOM Definition Flash or SOMATOM Force, Siemens Heathineers, Forchheim, Germany). Scan parameters for the initial noncontrast enhanced coronary artery calcium scoring scan were as follows: 32×1.2 mm collimation, 120 kV tube voltage, 75 mA tube current, 3 mm slice thickness in a 1.5 mm increment (first and second generation DSCT scanners); 44×1.2 mm collimation, 120 kV tube voltage, 80 mA tube current, 3 mm slice thickness in a 1.5 mm increment (third generation DSCT scanner). Patients who were scanned using the first generation DSCT underwent a retrospectively ECG-gated contrast-enhanced cCTA acquisition with the following parameters: 100 to 120 kV tube potential adapted to the patient's body mass index, 350 to 650 mAs tube current-time product, 0.28 seconds gantry rotation time, $2 \times 32 \times 0.6$ mm detector collimation with z-flying focal spot technique. A biphasic contrast injection protocol was used to administer 70 to 90 ml of contrast medium (Ultravist, 370 mgI/ml iopromide, Bayer, Wayne, New Jersey) at 4 to 6 ml/sec, followed by a 30 ml saline flush. For the second generation DSCT system a prospectively ECG-gated contrast enhanced cCTA acquisition with the following parameters was used: 80 to 120 kV tube potential adapted to the patient's body mass index, 350 to 650 mAs tube current-time product, 0.28 seconds gantry rotation time, $2 \times 64 \times 0.6$ mm detector collimation with a z-flying focal spot. 50 to 80 ml of iodinated contrast material (370 mgI/ml iopromide) was injected at

4 to 6 ml/sec followed by a 30 ml saline bolus chaser. Patients scanned using the third generation DSCT system underwent a prospectively ECG-gated contrast enhanced cCTA acquisition with the following parameters: 70 to 130 kV tube potential automatically selected using an automated tube-voltage selection algorithm (CARE kV, Siemens), 200 to 650 mAs tube current-time product, 0.25 seconds gantry rotation time, $2 \times 96 \times 0.6$ mm detector collimation with a z-flying focal spot. Contrast enhancement was achieved by injecting 40 to 70ml iopromide at 4 to 6 ml/sec followed by a 30 ml saline bolus chaser. Beta blockers and nitroglycerine were used at the discretion of the attending physician. Filtered back projection image reconstruction was performed in the cardiac phase with the least motion: temporal resolution of 83, 75, or 66 ms, section thickness of 0.75 mm, reconstruction increment of 0.4 or 0.5 mm and a smooth convolution kernel (B26f). To calculate the effective radiation dose the dose-length-product was multiplied with a chest-specific conversion coefficient ($k = 0.014$ mSv/Gy/cm). cCTA data were analyzed on a postprocessing workstation (syngo.via VB10, Siemens). Two observers experienced in cCTA analysis who were blinded to the patients' history analyzed the lesion characteristics with consensus interpretation for all discordant cases. Transverse sections and automatically generated curved multiplanar reformations were assessed. For reference diameter and area stenosis determination, average dimensions of nonaffected vessel segments immediately proximal and distal to the lesion of interest were measured at points free of atherosclerotic plaque. Stenosis assessment was performed using the coronary artery disease reporting and data system (CAD-RADS). Obstructive CAD was defined as ≥50% stenosis.[10] A dedicated semiautomatic software prototype was used for the plaque quantification, (Coronary Plaque Analysis 2.0.3 syngo.via FRONTIER, Siemens Healthineers) as previously described.[11,12] Lesion length, total plaque volume, calcified, and noncalcified plaque volume were automatically measured by the software. The cut-off values (HU) used by the analysis software were as follows: lipid-rich (17 to 70), fibrotic (71 to 124), vessel lumen (125 to 511), and calcified (>511).[13] Presence of low attenuation plaque (<30 HU) was recorded. Plaque burden (PB in %) was measured as follows: PB = [plaque area/vessel area] x 100. Remodeling index (RI) was measured on vessel cross sections as the ratio of the vessel area of the lesion over the proximal luminal reference area.[14] The napkin-ring sign was assessed as a low attenuation plaque core surrounded by a circumferential area of higher attenuation.[15] Spotty calcifications were visually assessed as calcifications comprising <90° of the vessel circumferences and >3 mm length.[16] In cases that patients had a single significant stenosis and suffered MACE, this lesion was considered to be the MACE-related lesion. In patients with multiple lesions showing >50% luminal narrowing, the MACE-lesion was identified using either autopsy results (in case of cardiac death), findings on electrocardiography, wall motion abnormalities presented on echocardiography, or angiographic appearance during ICA as reported previously.[17]

CT-FFR was computed using a machine-learning based software prototype (Siemens cFFR, Version 2.1, Siemens, currently not commercially available) as previously

described.[7,18] This algorithm is used on a regular workstation and allows for the physician-driven creation of a patient-specific anatomical model of the coronary tree using a semiautomatic approach. The algorithm is based on a deep learning framework to integrate the complex nonlinear relation between the various features extracted from the coronary tree geometry and to compute the functional severity of the lesion. The deep learning algorithm employs a multilayer neural network architecture that was trained offline against a computational fluid dynamics simulation to learn the complex relation between the anatomy of the coronary tree and its corresponding hemodynamics. Based on geometric features (i.e., vessel radius, degree of tapering, and branch length) of the patient's coronary anatomy on cCTA, the algorithm uses the learned relation to calculate machine learning based CT-FFR values. The measurement of interest, for example FFR, is represented by a model built from a database of samples with known characteristics and outcomes derived from the computational fluid dynamic approach. For any point available within the coronary tree, CT-FFR was generated by computing the ratio of the average local pressure over a cardiac cycle to the average aortic pressure, resulting in a color-coded 3-dimensional mesh allowing for the determination of the CT-FFR value at arbitrary locations. Lesion-specific ischemia was defined as CT-FFR ≤0.80 as previously described.[19] ICA was performed as per current guidelines[20] by experienced interventional cardiologists. Each coronary segment was visually evaluated and quantitative coronary angiography measurement was performed. Additional invasive FFR measurements were performed at the discretion of the attending cardiologist with FFR ≤0.80 indicating lesion-specific ischemia.

MedCalc (MedCalc Software, version 15, Ostend, Belgium) was used for all statistical analyses. Continuous variables are displayed as mean ± standard deviation or median with interquartile range (IQR) when not normally distributed. Normal distribution was assessed using Kolmogorov-Smirnov testing. Student t Test and Mann-Whitney *U* test were used for parametric or non0parametric data, respectively. A multivariable logistic regression analysis was performed with cCTA-derived markers and CT-FFR as independent variables for the identification of MACE. Variables that were significant in a univariate analysis were entered into the multivariable logistical regression model. A receiver-operating characteristics (ROC) analysis was used to detect MACE. The area under the ROC curve (AUC) was measured according to the method of DeLong[21] for the evaluation of discriminatory power. The Youden index derived from ROC curve analysis was used for the optimal threshold. Sensitivity, specificity, positive predictive value and negative predictive value were measured and presented with a 95% confidence interval. In a stepwise fashion ROC curves were used to evaluate the prognostic value of ≥50% stenosis on cCTA, combination of plaque markers, and CT-FFR for MACE prediction. Model performance of increasing numbers of predictors was compared using the Wald test. Statistical significance was assumed with a p value ≤0.05.

Results

In this single-center retrospective study, data of a total of 82 patients (60 ± 11 years, 62% men) with 101 coronary narrowings who underwent cCTA and ICA and were followed up to 36 months for the occurrence of MACE were retrospectively analyzed. A flow chart of the study is illustrated in Figure 1. Additional baseline characteristics and results are shown in Table 1. After a median follow-up of 18.5 months (IQR 11.5 to 26.6), the composite end point of MACE was observed in 18 patients (21%). Two patients deceased from cardiac deaths, 16 suffered from recurrent acute coronary syndrome (ACS) (3 ST-segment elevation MI, 8 unstable angina pectoris, and 5 non-ST-segment elevation MI), which resulted in 14 late revascularization procedures. Two patients died from noncardiac reasons which resulted in an all-cause mortality of 4 patients (4.8%). Data was not available for 4 patients, thus they were lost to follow-up. MACE-related lesions showed a median CT-FFR value of 0.70 (IQR 0.64 to 0.80) with 11 of 18 lesions showing hemodynamic significant CAD based on CT-FFR. Fifteen lesions demonstrated obstructive CAD (stenosis ≥50%). Characteristics of MACE-related lesions and controls are described in more detail in Tables 1 and 2. In terms of plaque markers, lesion length, calcified plaque volume, noncalcified plaque volume, low attenuation plaque (<30 HU), and RI were significantly different in MACE-lesions compared with control lesions (all p <0.05) (Table 3). Likewise, stenosis ≥50% on cCTA (83% vs 65%, p = 0.015), and CT-FFR ≤0.80 (78% vs 29%, p = 0.0001) were significantly higher in MACE lesions than in the control group lesions. However, total plaque volume (147 vs 124 mm³) and overall plaque burden (66% vs 55%) showed no relevant differences between MACE lesions in comparison to control lesions (both p >0.05). In MACE lesions the prevalence of Napkin-ring sign was 67% compared with control lesions with 33% (p = 0.032) (Table 3). In multivariable logistics regression analysis, narrowing length >22.3 mm (odds ratio [OR] 1.17, p = 0.018), low attenuation plaque (<30 HU) (OR 4.59, p = 0.003), Napkin ring sign (OR 2.71, p = 0.034), stenosis ≥50% on cCTA (OR 3.83, p = 0.042), and CT-FFR ≤0.80 (OR 7.79, p = 0.001) were significant predictors for MACE. Sensitivity, specificity, positive predictive value, and negative predictive value derived from ROC curve analysis with the optimal thresholds of plaque markers to identify MACE are shown in Table 4. A case example of coronary stenosis on cCTA, cCTA-based plaque analysis, CT-FFR determination, and ICA is illustrated in Figure 2. For markers demonstrating significant differences between MACE-lesions and control lesions in univariate analysis, a stepwise model of ROC curves was performed to evaluate the predictive value of combination of markers for MACE. A combined approach of plaque markers (lesion length, RI, noncalcified plaque volume, calcified plaque volume, napkin ring sign, and low attenuation plaque) added to stenosis ≥50% on cCTA (AUC 0.60) yielded in an improved value over stenosis ≥50% on cCTA alone (AUC 0.87, p = 0.0001). With the addition of CT-FFR ≤0.80 to stenosis ≥50% on cCTA + plaque markers the predictive value was further improved with incremental discriminatory power (AUC 0.94, p = 0.042; Figure 3).
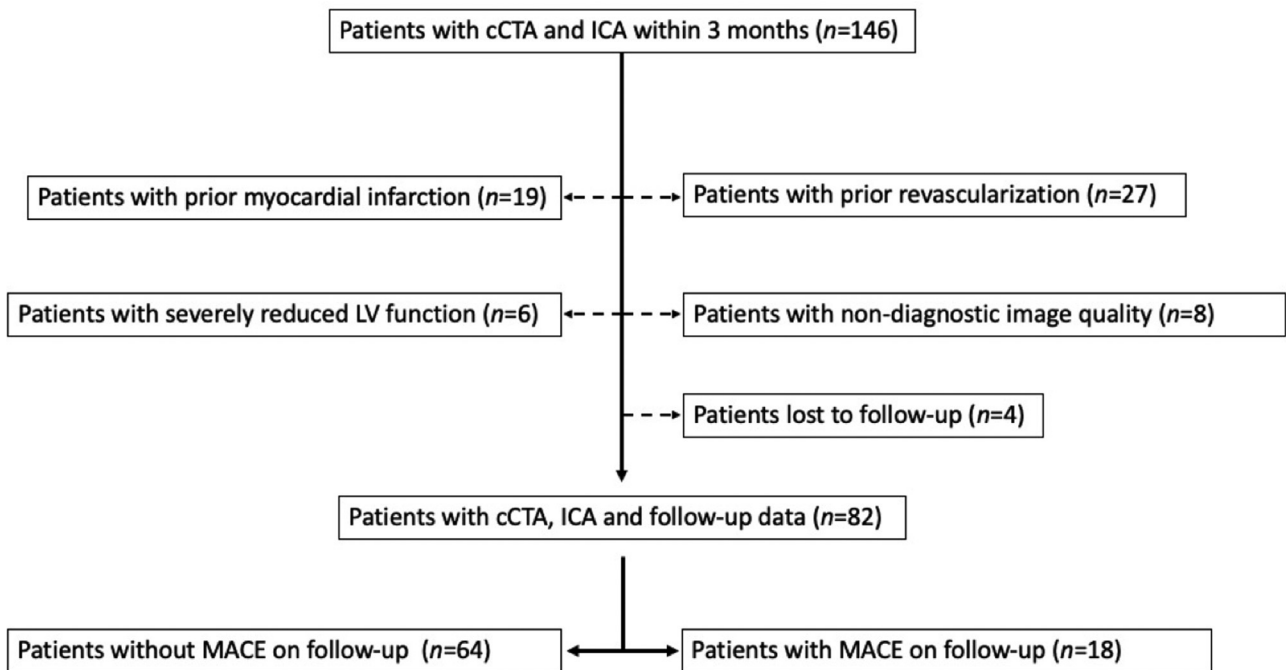
Figure 1. Flow chart of the study.

Table 1
Patient demographics. Total patient cohort (n = 82)

Parameter	All patients (n = 82)	MACE		p Value
		Yes (n = 18)	No (n = 64)	
Age (years)	60 ± 11	63 ± 13	60 ± 10	0.42
Men	51 (62%)	10 (56%)	41 (64%)	0.47
Height (cm)	172 ± 11	170 ± 9	172 ± 11	0.42
Weight (kg)	87 ± 19	88 ± 21	86 ± 19	0.85
Body mass index (kg/m^2)	30 ± 6	31 ± 7	29 ± 6	0.69
Hypertension*	57 (70%)	14 (78%)	43 (67%)	0.38
Diabetes mellitus[†]	26 (32%)	12 (30%)	7 (18%)	0.07
Dyslipidemia[‡]	42 (51%)	11 (61%)	11 (17%)	0.32
Smoker	22 (27%)	2 (11%)	20 (31%)	0.09
CAD family history	26 (32%)	11 (61%)	15 (23%)	0.33
Framingham risk score (%)	19 ± 10	21 ± 8	22 ± 10	0.77
Medication				
Aspirin	23 (28%)	4 (22%)	19 (%)	0.60
Statins	34 (41%)	8 (44%)	26 (41%)	0.72
Beta-blocker	26 (31%)	7 (39%)	19(30%)	0.41
Antidiabetics	26 (31%)	10 (55%)	16 (25%)	0.09
Diuretics	18 (22%)	6 (33%)	12 (19%)	0.62
ACE inhibitors	31 (38%)	7 (39%)	24 (38%)	0.12

CAD = coronary artery disease; ACE = angiotensin-converting enzyme.

* Defined as blood pressure >140 mm Hg systolic, >90 mm Hg diastolic, or use of antihypertensive medication.

[†] Defined as an HbA1c of ≥6.5% or use of anti-diabetic medication.

[‡] Defined as a total cholesterol of >200mg/dl or use of lipid lowering medication. Data presented as mean ± standard deviation or numbers with percentages (%).

Discussion

Our results show that cCTA-derived plaque markers and CT-FFR carry predictive value to identify adverse cardiac outcome and significantly improve the prognostic value beyond stenosis grading alone with increased discriminatory power. Especially the combined approach of applying plaque features together with CT-FFR determination yielded incremental predictive value for MACE (AUC 0.94 vs 0.60). In line with previous studies we showed that several morphological and functional cCTA-derived plaque markers are significantly different in lesions related with MACE compared with control lesions.[1,22] We observed that in terms of morphological plaque features, noncalcified plaque volume and the presence of low attenuation plaque

Table 2

Procedural results (82 patients with 101 coronary lesions)

Parameter	All lesions (n = 101)	MACE narrowings (n = 18)	Control narrowings (n = 83)	p Value
Left anterior descending artery	69 (68%)	9 (50%)	60 (72%)	0.47
Left circumflex artery	17 (17%)	5 (28%)	12 (14%)	0.56
Right coronary artery	15 (15%)	4 (22%)	11 (13%)	0.24
Proximal lesions	30 (30%)	5 (27%)	25 (30%)	0.72
Medial lesions	52 (51%)	8 (44%)	44 (53%)	0.35
Distal lesions	19 (19%)	5 (28%)	14 (17%)	0.28
FFR ≤0.80	34 (34%)	11 (61%)	23 (28%)	0.02
		MACE		
Parameter	*All patients (n = 82)*	*Yes (n = 18)*	*No (n = 64)*	*p value*
Heart rate (bpm)	68 ± 12	68 ± 11	68 ± 13	0.62
Dose-length-product (mGy*cm)	473 ± 53	473 ± 53	475 ± 52	0.72
Effective radiation dose (mSv)	6.4 ± 0.8	6.5 ± 0.7	6.4 ± 0.3	0.68

Data presented as mean ± standard deviation, numbers with percentages (%) or as medians with 25th and 75th percentile.

Table 3

Analysis of cCTA-derived plaque markers and CT-FFR for the prediction of MACE

Parameter	All lesions (n = 101)	MACE lesions (n = 18)	No MACE lesions (n = 83)	p Value
Lesion length (mm)	21 (17, 26)	24 (21, 26)	20 (16, 25)	0.008
Total plaque volume (mm^3)	135 (78, 173)	147 (94, 222)	124 (77, 171)	0.28
Calcified plaque volume (mm^3)	6.5 (3, 10)	3.5 (2, 8)	8 (3, 11)	0.019
Non-calcified plaque volume (mm^3)	120 (84, 162)	143 (97, 263)	114 (93, 144)	0.02
Plaque burden (%)	57 (42, 72)	66 (48, 73)	55 (42, 72)	0.21
Low attenuation plaque (<30HU)	30 (30%)	9 (50%)	21 (25%)	0.041
Remodeling index	1.06 (0.95, 1.15)	1.1 (1.05, 1.23)	1.04 (0.96, 1.15)	0.002
Napkin ring sign	39 (39%)	12 (67%)	27 (33%)	0.032
Spotty calcification	43 (43%)	10 (56%)	33 (40%)	0.22
Agatston calcium score	439 (190, 1068)	378 (84.0, 1075)	499 (222, 1059)	0.60
Stenosis ≥50%	69 (68%)	15 (83%)	54 (65%)	0.015
CT-FFR value	0.85 (0.74, 0.92)	0.70 (0.64, 0.80)	0.88 (0.77, 0.93)	<0.0001
CT-FFR ≤0.80	38 (38%)	11 (78%)	24 (29%)	0.0001

Data presented as medians with 25th and 75th percentile in parentheses or percentages in parentheses (%).

Table 4

Diagnostic performance of cCTA-derived plaque markers and CT-FFR for the prediction of MACE

Parameter	Sensitivity	Specificity	PPV	NPV
Lesion length >22.3 mm	72% (47%-90%)	72% (61%-82%)	36% (27%-47%)	92% (85%-96%)
Noncalcified plaque volume >195 mm^3	36% (19%-56%)	94% (87%-98%)	72% (46%-88%)	79% (74%-84%)
Calcified plaque-volume ≤9.1 mm^3	82% (63%-94%)	42% (31%-55%)	35% (30%-42%)	86% (73%-94%)
Low attenuation plaque (<30 HU)	57% (34%-78%)	76% (67%-86%)	40% (29%-54%)	87% (81%-92%)
Remodeling index >1.04	71% (51%-87%)	52% (40%-64%)	36% (29%-44%)	83% (72%-90%)
Napkin ring sign	68% (48%-84%)	56% (44%-68%)	37% (29%-46%)	82% (72%-89%)
Stenosis ≥50%	89% (72%-98%)	31% (21%-44%)	33% (29%-38%)	88% (71%-96%)
CT-FFR ≤0.80	82% (63%-94%)	79% (68%-88%)	61% (49%-72%)	92% (84%-96%)

PPV = positive predictive value; NPV = negative predictive value. Data presented as percentages (%) with 95% confidence intervals in parentheses.

were significantly higher in MACE-related lesions. Whereas it is well-known that noncalcified plaques and especially low attenuation plaques are at increased risk for future events,[23] we found the calcified plaque volume to be lower in MACE lesions compared with control lesions in our current investigation, which may support the assumption that calcification may have an important impact on plaque stabilization.[17] The occurrence of low attenuation plaque, the presence of Napkin ring sign (67% vs 33%, p = 0.032) and elevated RI (1.1 vs 1.04, p = 0.002), are known as so called "high risk plaque features." These markers were significantly more frequent in MACE lesions versus control lesions. A factum that has also been shown by Motoyama et al who demonstrated association of these risk markers with cardiac events.[24] However, while Yamamoto et al showed prognostic value of spotty calcifications in the "PREDICT Study"[4] this marker failed to show differences between MACE lesions and controls (56% vs 40%, p = 0.22) in our study. Logistic regression analysis
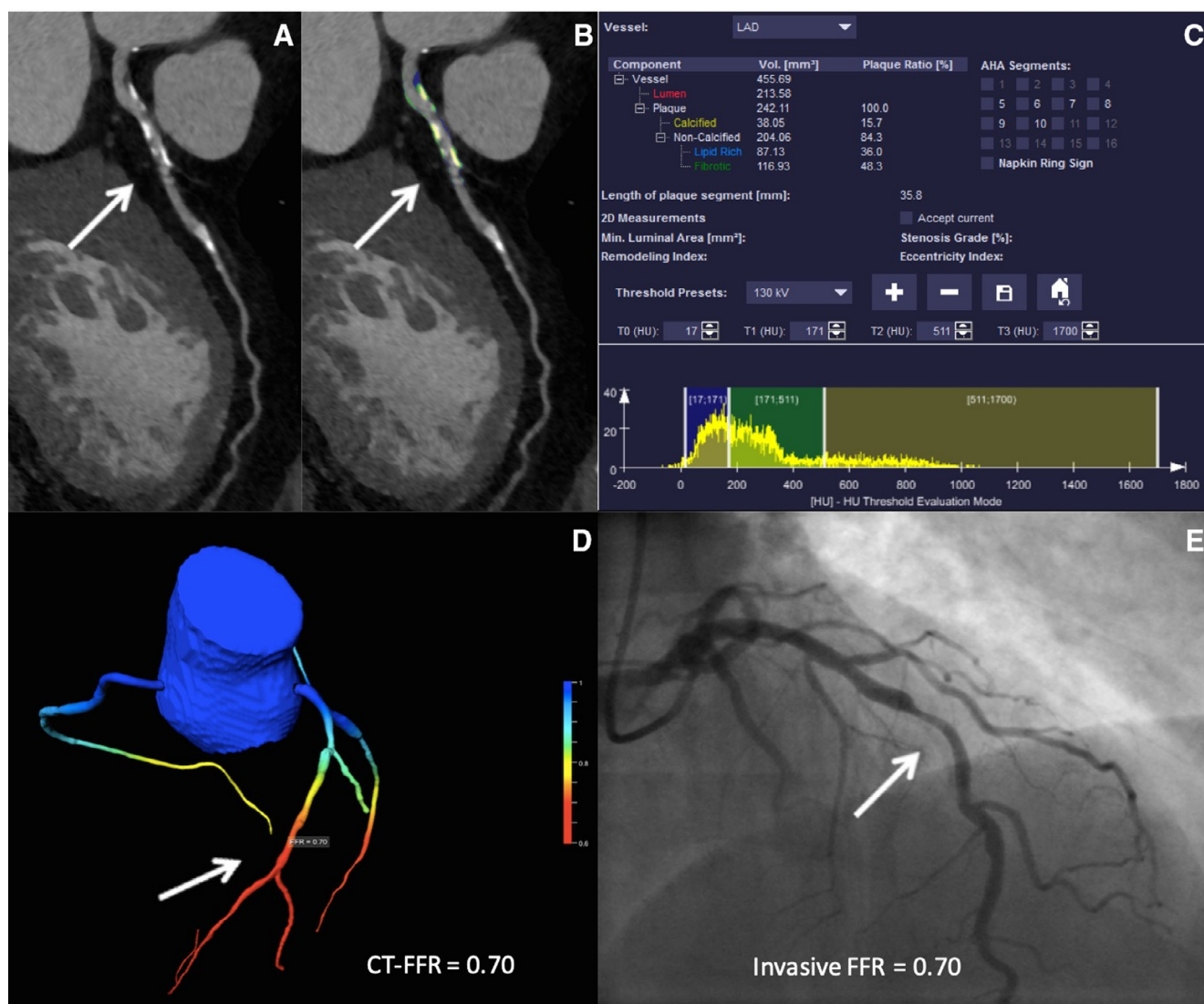
Figure 2. Case example of coronary stenosis on cCTA, cCTA-based plaque analysis, CT-FFR determination, and ICA. Sixty-six year old man who underwent cCTA for suspected CAD. (*A*) cCTA demonstrated mainly calcified plaques in the proximal LAD (arrow). (*B, C*) Color-coded semiautomatic plaque quantification of the lesion shows the plaque composition (mainly calcified). (*D*) Three-dimensional color-coded mesh reveals a CT-FFR value of 0.77, indicating lesion-specific ischemia (*arrow*). (*E*) ICA on index hospitalization shows only moderate stenosis of the LAD (*D, arrow*). The patient was readmitted 6 months after the initial cCTA with unstable angina and underwent late percutaneous coronary revascularization.

identified lesion length (OR 1.17, p = 0.018), low attenuation plaque (OR 4.59, p = 0.003), and Napkin ring sign (OR 2.71, p = 0.034) to have predictive value to detect MACE. Our results are consistent with previous findings by Bittner et al who demonstrated that high risk plaque components have predictive value to identify the occurrence of adverse cardiac events.[25] We found that not only obstructive CAD on cCTA (stenosis ≥50%, OR 3.83, p = 0.042) but also and more importantly CT-FFR ≤0.80 (OR 7.79, p = 0.001) as a marker of hemodynamic significance of CAD showed high discriminatory value to differentiate between MACE lesions and controls. Furthermore, machine-learning based CT-FFR demonstrated higher discriminatory value over cCTA and plaque markers. The combined approach of anatomical stenosis grading with the addition of plaque characteristics showed superior value over stenosis assessment alone. However, the addition of CT-FFR analysis to visual stenosis

grading on cCTA and plaque quantification resulted in incremental predictive value (AUC 0.94, p = 0.042). A previous investigation performed by Duguay et al[26] revealed CT-FFR to be a better predictor than stenosis grading on ICA for the identification of future MACE in the setting of nonculprit coronary lesions in index ACS. However, the composition of coronary plaques was not assessed by the authors of that study. Information derived from coronary plaque quantification may further inform patient treatment decision making and allow for sufficient risk stratification and subsequent lifestyle modification. Although there is robust data on the value of plaque quantification and characterization for sufficient risk stratification beyond stenosis grading on cCTA alone, the manual or semiautomated plaque analysis is rather time-consuming and requires manual adjustment. Thus, fully automated or machine-learning based applications incorporating big data derived from cCTA will most likely guide the
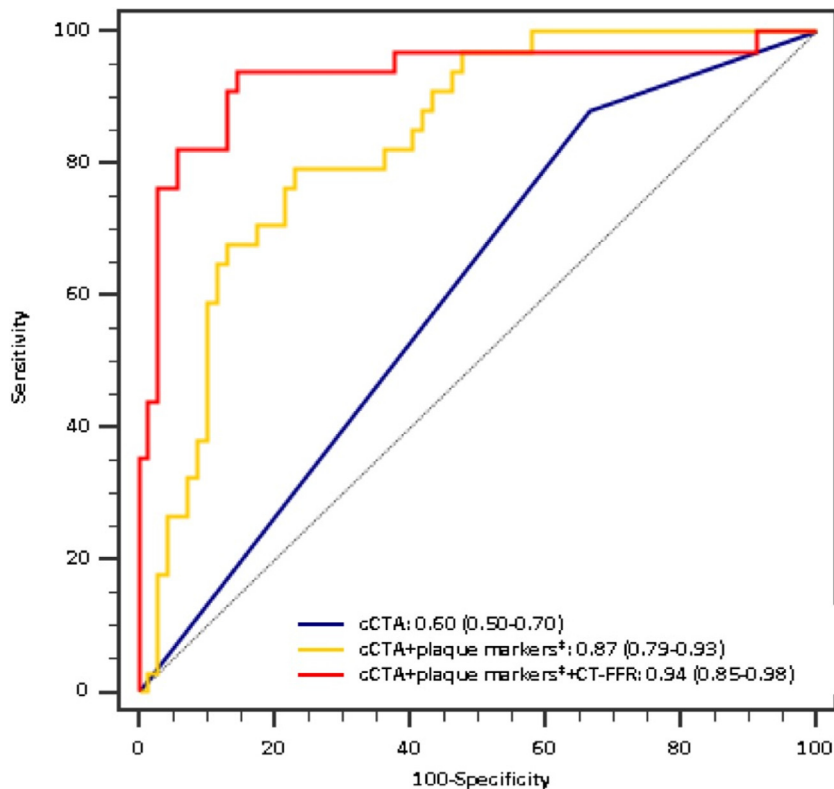
Figure 3. Comparison of different models for the prediction of MACE. Stepwise model of receiver operating characteristic (ROC) curves for cCTA-derived plaque markers including ≥50% stenosis and CT-FFR. Model 1 comprises ≥50% stenosis alone (*blue line*) with an area under the curve (AUC) of 0.60, Model 2 contains ≥50% stenosis + plaque markers* with an AUC of 0.87, p = 0.0001 (*yellow line*), and Model 3 incorporated Model 2 + CT-FFR resulting in the highest predictive value with an AUC of 0.94, p = 0.042 (*red line*). *Plaque markers: lesion length, remodeling index, noncalcified plaque volume, calcified plaque volume, napkin ring sign, and low attenuation plaque. (Color version of figure is available online.)

future of cardiac imaging.[27] In addition, with CT-FFR this combined anatomical and morphological information will provide more insight into clinical decision making of CAD and outcome prediction. Some limitations of this study need to be addressed. We present a retrospective single-center study with a relatively small number of patients included which may incur selection bias. Therefore, larger studies will be necessary to validate our findings. Our results on multivariate analysis may be underpowered by the limited number of observations per variable included.[28] Thus, this data should only be considered hypothesis generating. Additionally, plaque quantification was not performed in patients with ACS caused by ST-elevation MI, as these patients directly undergo ICA without previous cCTA. Only patients with at least one invasively quantified stenosis by FFR were included. The identification of the MACE-related lesion on coronary CTA images has been thoroughly performed according to ICA findings. However, this could represent a bias for the accurate identification of MACE-related lesions. Furthermore, patient follow-up was performed using electronic medical records of the hospitals; therefore, we might have missed events occurring outside the hospital. Furthermore, we did not correlate our findings on cCTA with an invasive reference standard for intracoronary plaque assessment (such as intravascular ultrasound).

However, the semiautomated plaque software used in the present study has been established in previous studies.[11,29]

1. Min JK, Feignoux J, Treutenaere J, Laperche T, Sablayrolles J. The prognostic value of multidetector coronary CT angiography for the prediction of major adverse cardiovascular events: a multicenter observational cohort study. *Int J Cardiovasc Imaging* 2010;26:721–728.
2. De Cecco CN, Varga-Szemes A, Meinel FG, Renker M, Schoepf UJ. Beyond stenosis detection: computed tomography approaches for determining the functional relevance of coronary artery disease. *Radiol Clin North Am* 2015;53:317–334.

3. Cho I, Al'Aref SJ, Berger A, B OH, Gransar H, Valenti V, Lin FY, Achenbach S, Berman DS, Budoff MJ, Callister TQ, Al-Mallah MH, Cademartiri F, Chinnaiyan K, Chow BJW, DeLago A, Villines TC, Hadamitzky M, Hausleiter J, Leipsic J, Shaw LJ, Kaufmann PA, Feuchtner G, Kim YJ, Maffei E, Raff G, Pontone G, Andreini D, Marques H, Rubinshtein R, Chang HJ, Min JK. Prognostic value of coronary computed tomographic angiography findings in asymptomatic individuals: a 6-year follow-up from the prospective multicentre international CONFIRM study. *Eur Heart J* 2018;39:934–941.

4. Yamamoto H, Kihara Y, Kitagawa T, Ohashi N, Kunita E, Iwanaga Y, Kobuke K, Miyazaki S, Kawasaki T, Fujimoto S, Daida H, Fujii T, Sato A, Okimoto T, Kuribayashi S, Investigators P. Coronary plaque characteristics in computed tomography and 2-year outcomes: the PREDICT study. *J Cardiovasc Comput Tomogr* 2018;12:436–443.

5. Tesche C, De Cecco CN, Albrecht MH, Duguay TM, Bayer RR 2nd, Litwin SE, Steinberg DH, Schoepf UJ. Coronary CT angiography-derived fractional flow reserve. *Radiology* 2017;285:17–33.

6. Coenen A, Kim YH, Kruk M, Tesche C, De Geer J, Kurata A, Lubbers ML, Daemen J, Itu L, Rapaka S, Sharma P, Schwemmer C, Persson A, Schoepf UJ, Kepka C, Hyun Yang D, Nieman K. Diagnostic accuracy of a machine-learning approach to coronary computed tomographic angiography-based fractional flow reserve: result from the MACHINE Consortium. *Circ Cardiovasc Imaging* 2018;11:e007217.

7. Tesche C, De Cecco CN, Baumann S, Renker M, McLaurin TW, Duguay TM, Bayer RR 2nd, Steinberg DH, Grant KL, Canstein C, Schwemmer C, Schoebinger M, Itu LM, Rapaka S, Sharma P, Schoepf UJ. Coronary CT angiography-derived fractional flow reserve: machine learning algorithm versus computational fluid dynamics modeling. *Radiology* 2018;288:64–72. 171291.

8. Task Force on the management of STseamiotESoC, Steg PG, James SK, Atar D, Badano LP, Blomstrom-Lundqvist C, Borger MA, Di Mario C, Dickstein K, Ducrocq G, Fernandez-Aviles F, Gershlick AH, Giannuzzi P, Halvorsen S, Huber K, Juni P, Kastrati A, Knuuti J, Lenzen MJ, Mahaffey KW, Valgimigli M, van 't Hof A, Widimsky P, Zahger D. ESC guidelines for the management of acute myocardial infarction in patients presenting with ST-segment elevation. *Eur Heart J* 2012;33:2569–2619.

9. von Knebel Doeberitz PL, De Cecco CN, Schoepf UJ, Duguay TM, Albrecht MH, van Assen M, Bauer MJ, Savage RH, Pannell JT, De Santis D, Johnson AA, Varga-Szemes A, Bayer RR, Schonberg SO, Nance JW, Tesche C. Coronary CT angiography-derived plaque quantification with artificial intelligence CT fractional flow reserve for the identification of lesion-specific ischemia. *Eur Radiol* 2019;29:2378–2387.

10. Cury RC, Abbara S, Achenbach S, Agatston A, Berman DS, Budoff MJ, Dill KE, Jacobs JE, Maroules CD, Rubin GD, Rybicki FJ, Schoepf UJ, Shaw LJ, Stillman AE, White CS, Woodard PK, Leipsic JA. CAD-RADSTM Coronary Artery Disease - Reporting and Data System. An expert consensus document of the Society of Cardiovascular Computed Tomography (SCCT), the American College of Radiology (ACR) and the North American Society for Cardiovascular Imaging (NASCI). Endorsed by the American College of Cardiology. *J Cardiovasc Comput Tomogr* 2016;10:269–281.

11. Tesche C, Caruso D, De Cecco CN, Shuler DC, Rames JD, Albrecht MH, Duguay TM, Varga-Szemes A, Jochheim D, Baquet M, Bayer RR, Ebersberger U, Litwin SE, Chiaramida SA, Hoffmann E, Schoepf UJ. Coronary computed tomography angiography-derived plaque quantification in patients with acute coronary syndrome. *Am J Cardiol* 2017;119:712–718.

12. Tesche C, De Cecco CN, Caruso D, Baumann S, Renker M, Mangold S, Dyer KT, Varga-Szemes A, Baquet M, Jochheim D, Ebersberger U, Bayer RR 2nd, Hoffmann E, Steinberg DH, Schoepf UJ. Coronary CT angiography derived morphological and functional quantitative plaque markers correlated with invasive fractional flow reserve for detecting hemodynamically significant stenosis. *J Cardiovasc Comput Tomogr* 2016;10:199–206.

13. Voros S, Rinehart S, Qian Z, Joshi P, Vazquez G, Fischer C, Belur P, Hulten E, Villines TC. Coronary atherosclerosis imaging by coronary CT angiography: current status, correlation with intravascular interrogation and meta-analysis. *JACC Cardiovasc Imaging* 2011;4:537–548.

14. Achenbach S, Ropers D, Hoffmann U, MacNeill B, Baum U, Pohle K, Brady TJ, Pomerantsev E, Ludwig J, Flachskampf FA, Wicky S, Jang IK, Daniel WG. Assessment of coronary remodeling in stenotic and nonstenotic coronary atherosclerotic lesions by multidetector spiral computed tomography. *J Am Coll Cardiol* 2004;43:842–847.

15. Maurovich-Horvat P, Schlett CL, Alkadhi H, Nakano M, Otsuka F, Stolzmann P, Scheffel H, Ferencik M, Kriegel MF, Seifarth H, Virmani R, Hoffmann U. The napkin-ring sign indicates advanced atherosclerotic lesions in coronary CT angiography. *JACC Cardiovasc Imaging* 2012;5:1243–1252.

16. Park HB, Heo R, o Hartaigh B, Cho I, Gransar H, Nakazato R, Leipsic J, Mancini GB, Koo BK, Otake H, Budoff MJ, Berman DS, Erglis A, Chang HJ, Min JK. Atherosclerotic plaque characteristics by CT angiography identify coronary lesions that cause ischemia: a direct comparison to fractional flow reserve. *JACC Cardiovasc Imaging* 2015;8:1–10.

17. Pflederer T, Marwan M, Schepis T, Ropers D, Seltmann M, Muschiol G, Daniel WG, Achenbach S. Characterization of culprit lesions in acute coronary syndromes using coronary dual-source CT angiography. *Atherosclerosis* 2010;211:437–444.

18. Itu L, Rapaka S, Passerini T, Georgescu B, Schwemmer C, Schoebinger M, Flohr T, Sharma P, Comaniciu D. A machine-learning approach for computation of fractional flow reserve from coronary computed tomography. *J Appl Physiol (1985)* 2016;121:42–52.

19. Coenen A, Lubbers MM, Kurata A, Kono A, Dedic A, Chelu RG, Dijkshoorn ML, Gijsen FJ, Ouhlous M, van Geuns RJ, Nieman K. Fractional flow reserve computed from noninvasive CT angiography data: diagnostic performance of an on-site clinician-operated computational fluid dynamics algorithm. *Radiology* 2015;274:674–683.

20. Scanlon PJ, Faxon DP, Audet AM, Carabello B, Dehmer GJ, Eagle KA, Legako RD, Leon DF, Murray JA, Nissen SE, Pepine CJ, Watson RM, Ritchie JL, Gibbons RJ, Cheitlin MD, Gardner TJ, Garson A Jr., Russell RO Jr., Ryan TJ, Smith SC Jr. ACC/AHA guidelines for coronary angiography: executive summary and recommendations. A report of the American College of Cardiology/American Heart Association Task Force on Practice Guidelines (Committee on Coronary Angiography) developed in collaboration with the Society for Cardiac Angiography and Interventions. *Circulation* 1999;99:2345–2357.

21. DeLong ER, DeLong DM, Clarke-Pearson DL. Comparing the areas under two or more correlated receiver operating characteristic curves: a nonparametric approach. *Biometrics* 1988;44:837–845.

22. Cheruvu C, Precious B, Naoum C, Blanke P, Ahmadi A, Soon J, Arepalli C, Gransar H, Achenbach S, Berman DS, Budoff MJ, Callister TQ, Al-Mallah MH, Cademartiri F, Chinnaiyan K, Rubinshtein R, Marquez H, DeLago A, Villines TC, Hadamitzky M, Hausleiter J, Shaw LJ, Kaufmann PA, Cury RC, Feuchtner G, Kim YJ, Maffei E, Raff G, Pontone G, Andreini D, Chang HJ, Min JK, Leipsic J. Long term prognostic utility of coronary CT angiography in patients with no modifiable coronary artery disease risk factors: results from the 5 year follow-up of the CONFIRM International Multicenter Registry. *J Cardiovasc Comput Tomogr* 2016;10:22–27.

23. Versteylen MO, Kietselaer BL, Dagnelie PC, Joosen IA, Dedic A, Raaijmakers RH, Wildberger JE, Nieman K, Crijns HJ, Niessen WJ, Daemen MJ, Hofstra L. Additive value of semiautomated quantification of coronary artery disease using cardiac computed tomographic angiography to predict future acute coronary syndrome. *J Am Coll Cardiol* 2013;61:2296–2305.

24. Motoyama S, Kondo T, Sarai M, Sugiura A, Harigaya H, Sato T, Inoue K, Okumura M, Ishii J, Anno H, Virmani R, Ozaki Y, Hishida H, Narula J. Multislice computed tomographic characteristics of coronary lesions in acute coronary syndromes. *J Am Coll Cardiol* 2007;50:319–326.

25. Bittner DO, Mayrhofer T, Puchner SB, Lu MT, Maurovich-Horvat P, Ghemigian K, Kitslaar PH, Broersen A, Bamberg F, Truong QA, Schlett CL, Hoffmann U, Ferencik M. Coronary computed tomography angiography-specific definitions of high-risk plaque features improve detection of acute coronary syndrome. *Circ Cardiovasc Imaging* 2018;11:e007657.

26. Duguay TM, Tesche C, Vliegenthart R, De Cecco CN, Lin H, Albrecht MH, Varga-Szemes A, De Santis D, Ebersberger U, Bayer RRN, Litwin SE, Hoffmann E, Steinberg DH, Schoepf UJ. Coronary computed

tomographic angiography-derived fractional flow reserve based on machine learning for risk stratification of non-culprit coronary narrowings in patients with acute coronary syndrome. *Am J Cardiol* 2017;120:1260–1266.

27. Dey D, Slomka PJ, Leeson P, Comaniciu D, Shrestha S, Sengupta PP, Marwick TH. Artificial intelligence in cardiovascular imaging: JACC state-of-the-art review. *J Am Coll Cardiol* 2019;73: 1317–1335.

28. Kunce JT, Cook DW, Miller DE. Random variables and correlational overkill. *Educ Psychol Meas* 1975;35:529–534.

29. Tesche C, De Cecco CN, Vliegenthart R, Duguay TM, Stubenrauch AC, Rosenberg RD, Varga-Szemes A, Bayer RR 2nd, Yang J, Ebersberger U, Baquet M, Jochheim D, Hoffmann E, Steinberg DH, Chiaramida SA, Schoepf UJ. Coronary CT angiography-derived quantitative markers for predicting in-stent restenosis. *J Cardiovasc Comput Tomogr* 2016;10:377–383.